Focussed on: Fracture and Structural Integrity related Issues

Study of short cracks under biaxial fatigue

P. Lopez-Crespo, B. Moreno, A. Garcia-Gonzalez, J. Zapatero
Department of Civil and Materials Engineering, University of Malaga, C/Dr Ortiz Ramos s/n, 29071 Malaga, Spain
plopezcrespo@uma.es

A. Lopez-Moreno
Department of Materials Science and Metallurgy Engineering, University of Jaen, Campus Las Lagunillas 23071 Jaen, Spain

ABSTRACT. In this paper a methodology for evaluating crack initiation under biaxial conditions is presented. The methodology consists of evaluating the crack length automatically with digital processing of high-magnification images of the crack. The methodology was applied to study five different strain conditions on a low carbon ferritic-pearlitic steel specimen with tubular shape. A hole of 150 μm diameter was drilled to enforce the crack to initiate at a particular spot. Different combinations of axial and torsional strains were analysed during the initiation stage of the crack. The setup employed allowed detection of the crack to within 6 μm from the edge of the hole on average and monitoring of the crack during early stages. Fatigue crack propagation curves clearly showed oscillations due to microstructure. It was also observed that these oscillations decreased as the torsional component of the strain was increased.

KEYWORDS. Biaxial fatigue; Proportional loading; Fatigue crack growth; Crack initiation

INTRODUCTION

Understanding the behaviour of engineering components under biaxial load is crucial for a number of industries, including aerospace, automobile and power generation industries. Different models have been proposed in an attempt to characterise the behaviour under such conditions [1]. Stress-based models can be used to predict the fatigue life if the plastic strains are small [2]. Strain-based models are typically employed in the low-cycle fatigue regime where significant plasticity may occur [3]. Within strain-based models, critical plane approaches aim at predicting not only the fatigue life but also the crack direction of the crack [4, 5]. Energy models are based on evaluating the energy accumulated per cycle on the material, and use it as a damage parameter [6, 7]. Depending on the loading regime, an important portion of the life can be consumed in the initiation stage of the crack. Initiation stage includes crack nucleation and micro-crack growth up to a length of around 1 mm. During the initiation stage, the aforementioned models for predicting crack propagation under biaxial loads no longer can be applied, because they are based on continuum mechanics. The material microstructure and the surface morphology are critical to the crack growth during the initiation stage [8]. During the initiation, fatigue crack growth is different to that predicted by the above mentioned models, and oscillations are commonly observed on the growth curves. These are caused by grain and phase boundaries and other micro-structural features that continuum mechanics models do not take into account [9]. The current work aims at studying the fatigue crack growth behaviour of small cracks under different biaxial conditions.

MATERIAL AND SPECIMEN

A low carbon steel (St-52-3N) was examined in this investigation. This material is often employed in structural components. The composition of the steel is shown in Tab. 1. Fig. 1 shows a micrograph of the St-52-3N steel. Ferrite and pearlite bands can be seen in Fig. 1 as vertical bands in white and black respectively.

C	Si	Mn	P	S	Cr	Ni	Mo
0.17	0.225	1.235	0.010	0.0006	0.072	0.058	0.16

Table 1: Chemical composition in weight % of St-52-3N steel. The balance is Fe.

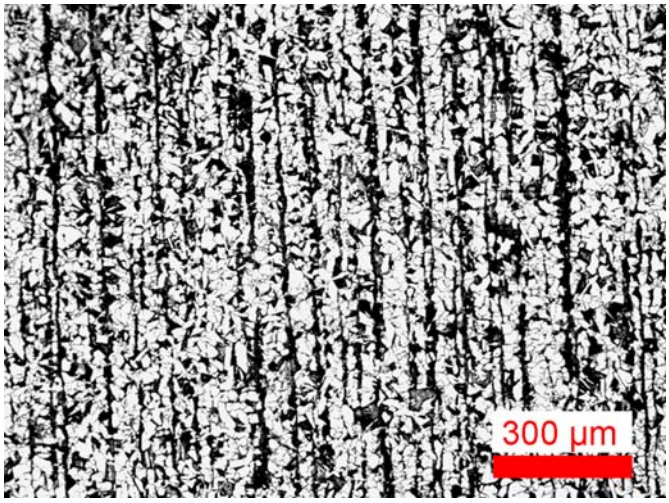

Figure 1: Optical micrograph of St-52-3N steel used in all tests.

Tubular hollow specimens were used in this work to apply different combinations of torsion and tensile loads. A schematic of the geometry is shown in Fig. 2. All experiments were conducted with MTS 809 servo-hydraulic loading rig, allowing different biaxial loads to be applied on the specimens. Biaxial extensometer Epsilon 3550 was used to measure axial and angular strains. All the crack measurements were made with a black and white 1.2 megapixel digital camera coupled to a long distance microscope. Co-axial illumination was used to acquire all images. Moreover, two additional LED 3 W lamps were also used to improve light distribution on the surface and remove reflections. Fig. 3 shows the setup employed in the experiment with all the different elements used.

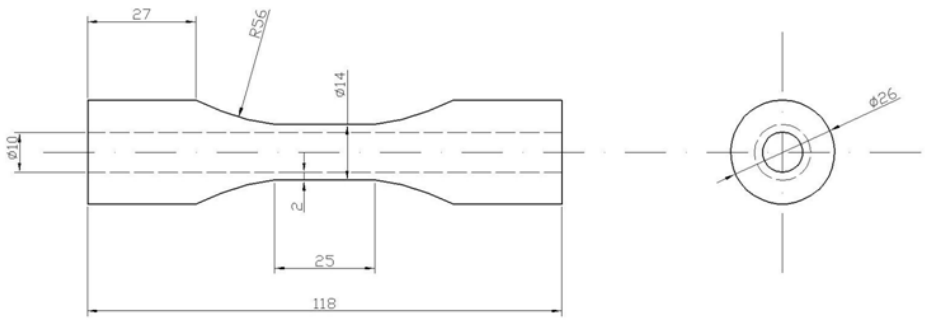

Figure 2: Geometry of the dog-bone shaped tubular hollow specimen used in the experiments. All dimensions are in mm.

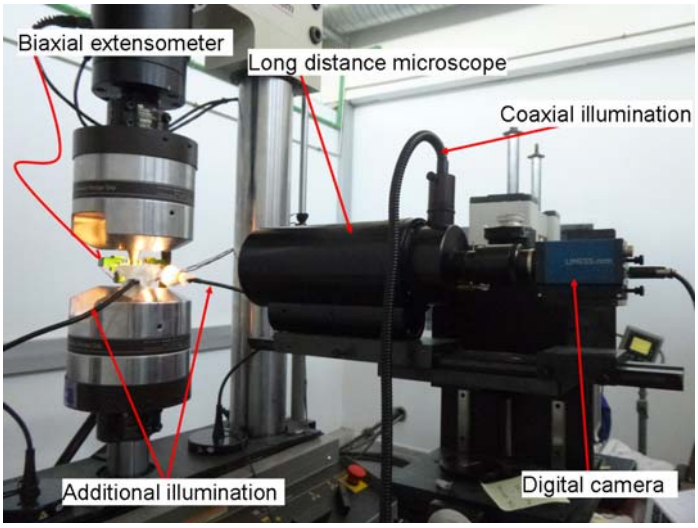

Figure 3: Experimental setup employed in this work.

EXPERIMENTS

The initiation stage of the crack growth was studied under combined proportional tension-compression and torsion tests [10]. All experiments were conducted under strain control mode with the help of the biaxial extensometer, with cyclic sinus signal with zero mean strain (R = -1). The aim of the work was to study a wide range of biaxial loads, with angle between shear and axial strains, φ, going from 0 to 90º in 15º increments (see Fig. 4). Imaging of the crack during initiation was possible by drilling a 150 μm diameter hole on the outer surface of the specimen [11]. The long-distance microscope was then focused on the hole, so that the crack initiation could be acquired. The hole on the surface looked like those shown in Fig. 5. The hole served as a stress raiser thus increasing the chances of the crack nucleating there. The size of the hole was chosen so that fatigue behaviour remains the same as that of the specimen without the hole, but large enough so that nucleation of the crack occurs at the hole. The hole influence on the fatigue life is negligible, as shown previously [12]. The setup allowed detection of the crack a few microns away from the edge of the hole. On average, detection of the crack was possible at distances of 6 μm from the edge of the hole. In practice, the crack did not nucleate at the hole in around 50% of the specimens tested. Only the samples where crack nucleated at the hole are reported here. When the shear component was increased beyond φ = 60º, it was not possible to nucleate the crack around the hole. Instead, the crack appeared either on the inside of the specimen or elsewhere. Consequently, it was not possible to conduct experiments with angle greater than φ = 60º. Tab. 2 summarises the different tension-compression and torsion strain combination studied.

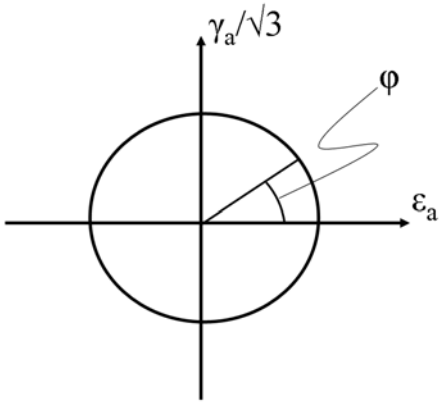

Figure 4: Definition of angle between axial and shear strain amplitudes.

Sample no.	φ (º)	ε_a	γ_a	N_f (cycles)
S1	0	0.005	0	875
S2	15	0.0048	0.022	950
S3	30	0.043	0.043	1400
S4	45	0.035	0.061	1850
S5	60	0.025	0.075	2425

Table 2: Summary of five samples employed in this work, showing the angle (φ) between axial strain amplitude (ε_a) and shear strain amplitude (γ_a), as well as the fatigue life (N_f) of each sample.

FATIGUE CRACK MEASUREMENTS

The setup described previously (Fig. 3) allowed acquisition of high-magnification images while the specimens were being strained. Magnification factor of 1.1 μm/pixel was achieved with working distance of approximately 380 mm, resulting in a field of view of 2 × 1.5 mm². In addition, the surface of the specimen was etched for 30 seconds with nitric acid diluted with ethanol to create a random pattern of the surface. This pattern can be used for obtaining displacement and strain fields with Digital Image Correlation (DIC). However, no DIC results are shown here and only the crack propagation results will be shown and discussed. Fig. 5 shows some examples of images acquired during the experiment.

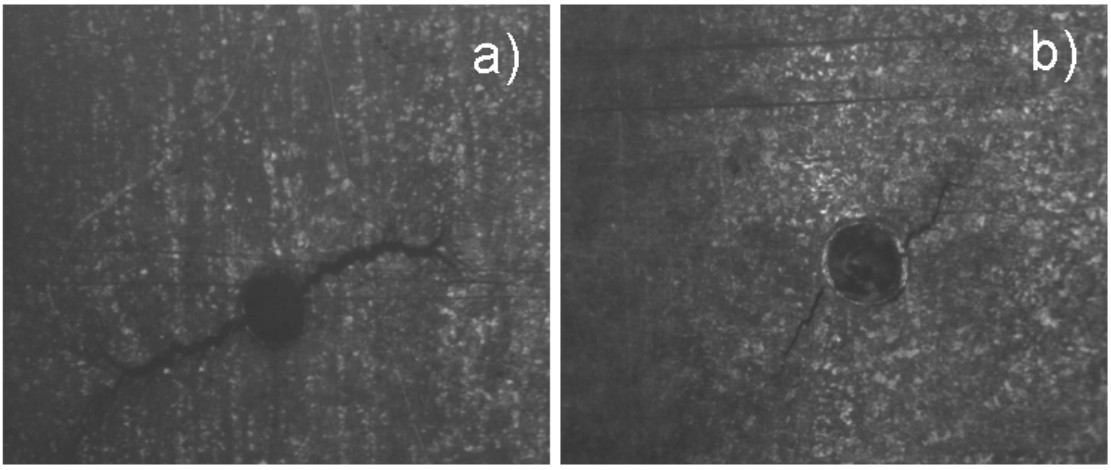

Figure 5: Images acquired for samples a) S2 and b) S4 after 950 and 1300 cycles respectively. The diameter of the hole in both images is 150 μm.

Around 120 images similar to those shown in Fig. 5 were acquired every 25 cycles. The image of maximum strain was then selected (Fig. 6.a) and analysed with an image processing algorithm. The algorithm evaluated the darkest pixels (minimum value in the grey scale) of the image and assumed they were inside the crack. Subsequently 20 grey values were added the minimum value to account for small intensity differences occurring within the crack. This information was employed for binarising the image, as has been done in previous works [13]. The binarised image was then analysed with an edge-finding routine to detect the edges which coincide with the crack edges (Fig. 6.b) [14, 15]. Finally, the detected crack was superimposed on the original image (Fig. 6.c). The algorithm allowed automatic evaluation of the crack length for all images acquired.

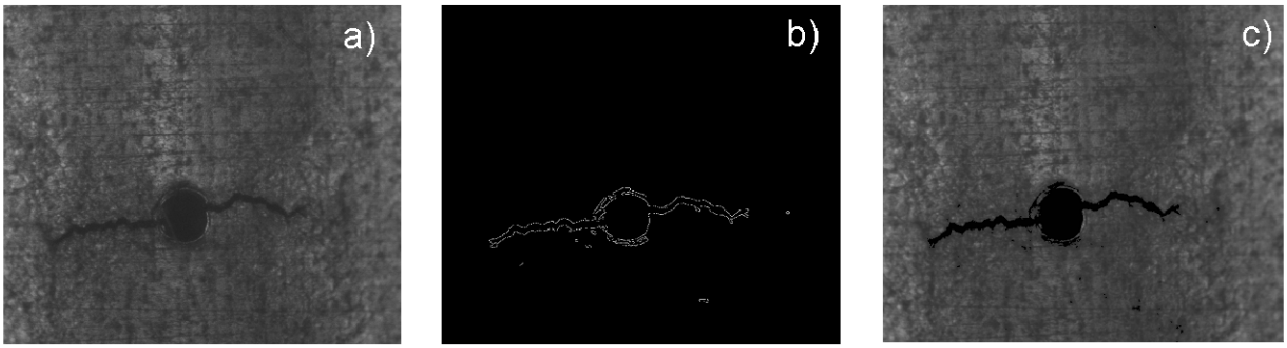

Figure 6: Image of sample S1 at maximum strain after applying 800 cycles. a) Raw image, b) image of the crack detected with the algorithm and c) detected crack superimposed on original image. The diameter of the hole is 150 μm.

The results of monitoring the crack length against the number of cycles during the early stages of the crack are shown in Fig. 7. The crack growth rates were computed from a-N curves by numerical differentiation following ASTM standard [16] and are shown in Fig. 8.

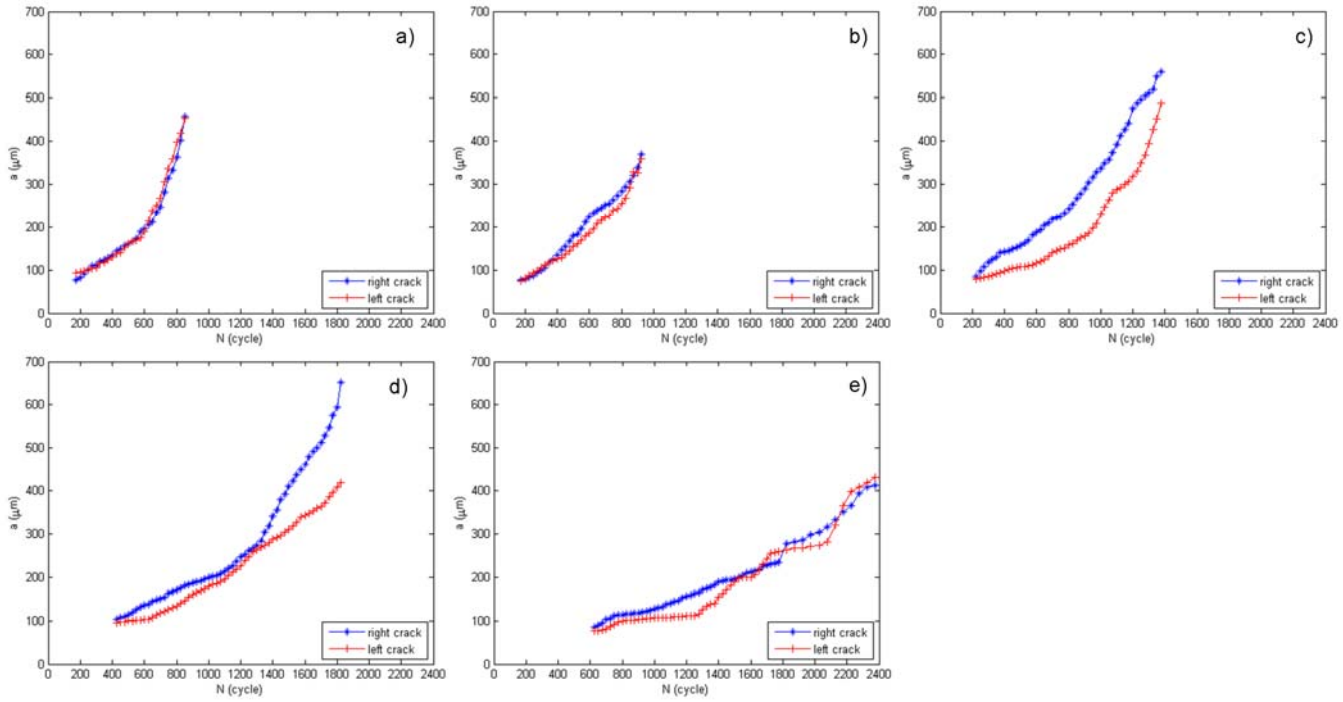

Figure 7: Crack length versus number of cycles for samples a) S1, b) S2, c) S3, d) S4 and e) S5.

Discussion

It is observed in Tab. 2 and Fig. 7 that fatigue lives increase from 875 to 2425 cycles as the angle φ increases from 0 to 60º. That is, for the strain ranges studied, increasing the shear component produces longer fatigue lives. Fig. 7 also shows that the growth of the cracks emanating to the right hand and left hand of the hole are similar for samples S1, S2 and S5. Differences between right and left cracks are observed for samples S3 and S4.

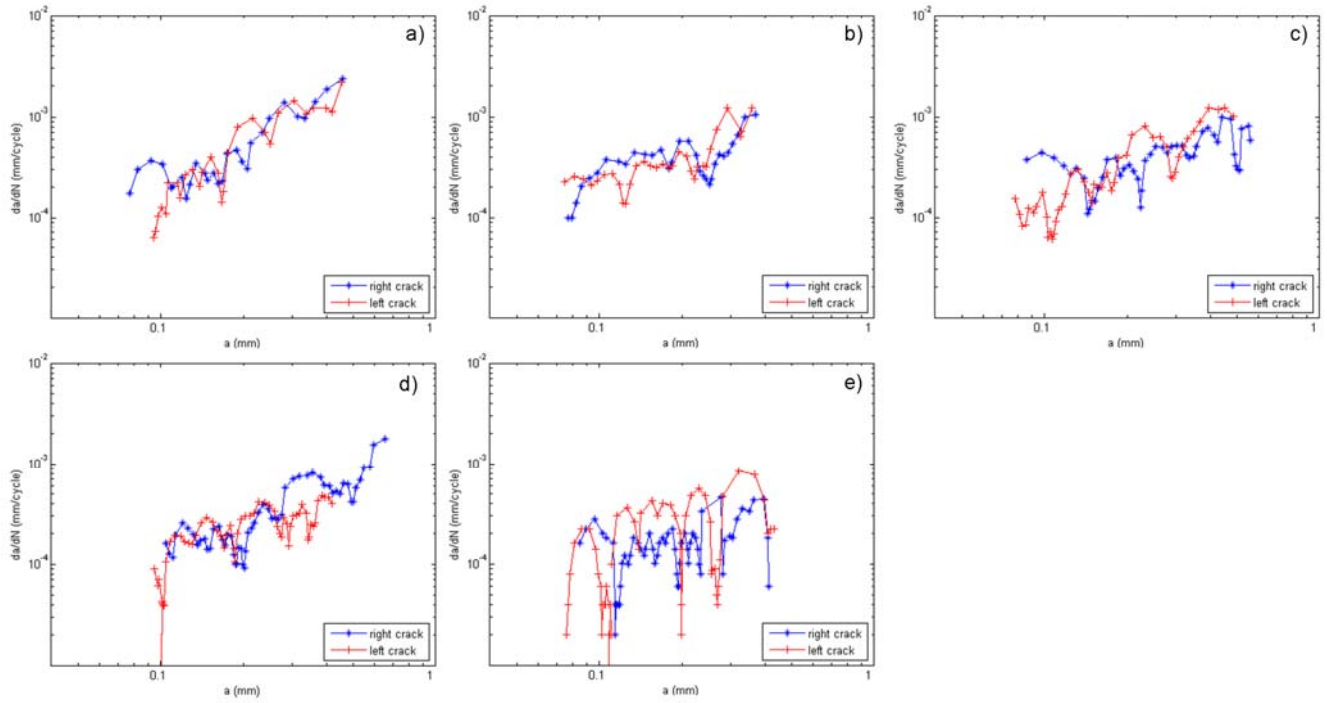

Figure 8: Fatigue crack propagation rates (da/dN) versus crack length for samples a) S1, b) S2, c) S3, d) S4 and e) S5.

Fig. 8 shows oscillations in the growth rate. These oscillations are due to microstructure and are often observed during crack initiation. The barrier effect is produced by the pearlite bands which are the phases with greatest strength [12]. Since the propagation rate curves are plotted on logarithmic scale, it is not easy to compare the magnitude of oscillations for the different angles. Thus the average oscillation for all angles was computed. The extent of each oscillation was obtained subtracting each local minimum to the subsequent local maximum. The average extent of the oscillations for all angles studied are shown in Fig. 9. These values are an estimate of how large acceleration and retardation transients are. Large oscillations are indicative of great accelerations and/or great retardations. It can be seen in Fig. 9 that acceleration and retardation transients increase as the angle φ decreases. That is, increasing the axial component of the strain produces stronger accelerations and retardations.

The more damaging effect of lower angle φ is evident from Fig. 7 since lower angles φ yield shorter fatigue lives. Accordingly, the combination of strains applied at lower angles φ (i.e. with higher tensile component) produces an overall higher level of stresses. Nevertheless, the current tests do not seem to follow the trend depicted by McDowell model (Fig. 10) [17, 18]. The model predicts higher level of oscillations as the load is increased. However, the data shown previously seems to follow a different trend. It is possible that increasing the torsional component, reduces the oscillations typically observed in small cracks and the effect of the torsional component is more pronounced than the mean stress effect. Nevertheless, further experiments should be conducted in order to evaluated both effects separately.

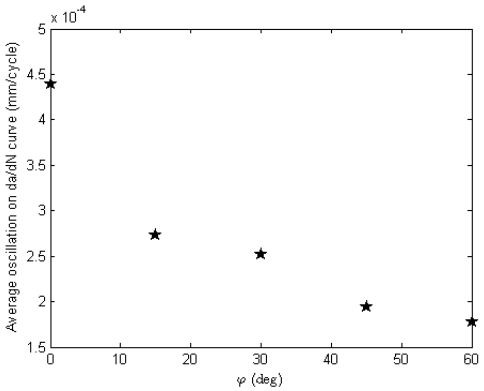

Figure 9: Average oscillation on da/dN curve for the five different angles, φ, studied.

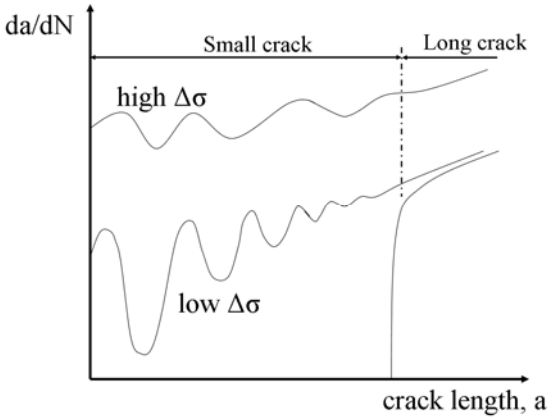

Figure 10: Typical evolution of crack growth rate as a function of crack length and stress amplitude. Adapted from [17].

CONCLUDING REMARKS

A methodology for characterising crack initiation under biaxial loading conditions has been described. It included automatic evaluation of crack length with digital processing algorithms and edge-finding routine. The setup allowed detection of the crack within 6 μm from the edge of a hole drilled so that the crack could be observed from its early stages. Different biaxial conditions were investigated in five tubular specimens of low carbon ferritic-pearlitic steel. Strains ranged from pure tension-compression axial strain to strain states with an increasing torsional component and a decreasing axial component. Typical oscillations with acceleration and retardation transients were observed throughout all the strains states studied. These oscillations were ascribed to grain or phase boundaries existing in the material. The retardations seem to appear when the crack meets a pearlite band. In addition, the magnitude of the oscillations decreases with increasing torsional component. It was not possible to correlate the different oscillation levels with previous models describing crack growth at the initiation stage.

ACKNOWLEDGEMENTS

Financial support of Junta de Andalucía through Proyectos de Excelencia grant reference TEP-3244 and of Spanish Ministerio de Economía y Competitividad through grant reference DPI2012-33382 is greatly acknowledged. Experimental help of Mr Pablo Cobos-Rodriguez and Mr Hector Martin is also greatly acknowledged.

REFERENCES

[1] You, B. R., Lee S. B., A critical review on multiaxial fatigue assessments of metals, International Journal of Fatigue, 18(4) (1996) 235-244.
[2] McDiarmid, D. L., A general criterion for high cycle multiaxial fatigue failure, Fatigue and Fracture of Engineering Materials and Structures, 14(4) (1991) 429-453.
[3] Socie, D. F., Marquis, G. B., Multiaxial Fatigue, Warrendale, PA (USA), Society of Automotive Engineers, Inc., (2000).
[4] Brown, M. W., Miller, K. J., A theory for fatigue under multiaxial stress-strain conditions, In: Proceedings of the Institution of Mechanical Engineers, 187 (1973) 745-755.
[5] Fatemi, A., Socie, D.. A Critical Plane approach to multiaxial fatigue damage including out-of-phase loading, Fatigue and Fracture of Engineering Materials and Structures, 11(3) (1988) 149-165.
[6] Garud, Y. S., A new approach to the evaluation of fatigue under multiaxial loadings, Journal of Engineering Materials and Technology, 103 (1981) 118-126.
[7] Ellyin, F., Kujawski, D., Amultiaxial fatigue criterion including mean-stress effect. In: ASTM STP 1191. McDowell DL, Ellis R, editors. West Conshohocken, (1993) 55-66.

[8] Suresh, S., Ritchie, R.O., Propagation of short fatigue cracks, International Materials Reviews, 29(1) (1984) 445-475.
[9] McDowell, D.L., Multiaxial small fatigue crack growth in metals, International Journal of Fatigue, 19 (1987) S127-S135.
[10] Lopez-Crespo, P., Moreno, B., Lopez-Moreno, A., Zapatero, J., Study of crack orientation and fatigue life prediction in biaxial fatigue with critical plane models, Engineering Fracture Mechanics, (2014) to appear.
[11] Moreno, B., Lopez-Crespo, P., Zapatero, J., High magnification crack-tip field characterisation under biaxial conditions, Frattura ed Integrità Strutturale, 25 (2013) 145-152.
[12] Lopez-Crespo, P., Moreno, B., Lopez-Moreno, A., Zapatero, J., Characterisation of crack-tip fields in biaxial fatigue based on high-magnification image correlation and electro-spray technique, International Journal of Fatigue, manuscript accepted (2014), http://dxdoiorg/101016/jijfatigue201402016.
[13] Withers, P. J., Lopez-Crespo, P., Kyrieleis, A., Hung, Y.-C., Evolution of crack-bridging and crack-tip driving force during the growth of a fatigue crack in a Ti/SiC composite, In: Proceedings of the Royal Society A, Mathematical, Physics & Engineering Sciences, (2012), doi: 101098/rspa20120070.
[14] Lopez-Crespo, P., Shterenlikht, A., Patterson, E. A., Withers, P. J., Yates, J. R., The stress intensity of mixed mode cracks determined by digital image correlation, Journal of Strain Analysis for Engineering Design, 43 (2008) 769-780.
[15] Lopez-Crespo, P., Burguete, R. L., Patterson, E. A., Shterenlikht, A., Withers, P. J., Yates, J. R., Study of a crack at a fastener hole by digital image correlation, Experimental Mechanics (2008).
[16] ASTM E647 Standard Test Method for Measurement of Fatigue Crack Growth Rates, (2003).
[17] McDowell, D. L., Bennett, V. P., A microcrack growth law for multiaxial fatigue, Fatigue and Fracture of Engineering Materials and Structures, 19(7) (1996) 821-837.
[18] McDowell, M. L., An engineering model for propagation of small cracks in fatigue, Engineering Fracture Mechanics, 56(3) (1997) 357-377.